Journal of Optics
https://doi.org/10.1007/s12596-024-02248-4

RESEARCH ARTICLE

Spectroscopic characterization of tin prepared by microwave technique

Maryam A. Hussein[1] · **Kadhim A. Aadim**[1]

Received: 31 August 2024 / Accepted: 9 September 2024

Abstract
In this study, a microwave induced plasma jet (MIPJ) system was used to generate a non-thermal plasma jet with a standard frequency of 2.45 GHz in the microwave power range of 800 W at atmospheric pressure. Argon (Ar) gas was flowed around the burner in an adjustable ratio using a flow meter and controller. The effects of the microwave induced plasma jet (MIPJ) parameters, including applied voltage and Ar flow rate, on the macroscopic MP parameters were investigated. The parameters examined included plasma frequency (w_{pe}), Debye length (λ_D), electron density (n_e), particle temperature (T_e), and number of particles (N_D). The spectral emission lines were analyzed and identified using the photometric method of emission spectroscopy. The results showed that the MPJ temperature decreased with increasing applied voltage, while an increase in the Ar-Ar gas flow ratio resulted in an increase in the Ar-Ar gas density, which led to an increase in the plasma frequency and Debye length. The nanoparticles were characterized using UV-Vis spectroscopy. The optical parameters of the samples showed a strong dependence on the average crystal size.

Keywords Microwave induced plasma jet · Optical emissions spectroscopy · Applied voltage · Argon gas · Optical parameters · Plasma parameters

Introduction

A plasma is an ionized gas, i.e. a collection of charged particles (ions and electrons), where the term ionized includes the presence of one or more free electrons [1]. Plasmas have free charged particles, with positive and negative charges being stored roughly in the macroscopic phase. This occurs when elements in a particular state of matter are heated to temperatures above thermal energy and well above the bonding temperature [2]. Due to the high electron temperatures in these plasmas, heavy particles, i.e. electrons, are connected, and although elastic collisions are less effective than heavy particle collisions, they can still transfer energy to other processes, such as activation and ionization or dissociation of molecules, which explains the great interest in these plasmas [3]. Microwave plasma technology is widely used in modern industrial applications, including material processing, surface treatment, sterilization and decontamination [4]. Microwave plasma torches are particularly versatile and can be operated with noble gases such as argon (Ar) and helium (He), as well as nitrogen (N2), oxygen (O2) and even ambient air. This versatility significantly expands their range of industrial applications. A key advantage of the microwave plasma torch is its high coupling efficiency (up to 90%), which effectively concentrates the microwave energy into the plasma within the short-circuited waveguide. This high efficiency is crucial for optimizing the energy transfer process as it ensures that most of the microwave power is effectively utilized, improving overall efficiency and reducing energy losses. The microwave plasma torch is an invention similar to the magnetron used in domestic microwave ovens. These magnetrons are inexpensive, numerous and compact. To operate the magnetron of a domestic microwave oven, a voltage (4 kV) with a frequency (w = 2.45 GHz) and an average power of approximately (1 kW) must be supplied to the cathode of the magnetron. A higher power voltage transformer is used to generate the voltage, which is then rectified using a half-wave voltage doubler circuit. In

✉ Maryam A. Hussein
mariam.a@sc.uobaghdad.edu.iq

✉ Kadhim A. Aadim
kadhim.aadim@sc.uobaghdad.edu.iq

[1] College of Science, Department of Physics, University of Baghdad, Baghdad, Iraq

Published online: 20 September 2024

other words, the magnetron operates at a frequency of 60 Hz (alternating current) [5]. The purpose of the optical emission spectrometer (OES) [6] is to collect data on the characteristics of the plasma [7]. The following Eq. (1) is used to obtain the electron temperature (Te) in the local thermodynamic equilibrium (LTE) in (eV) [8]. Te is given by [9]:

$$T_e = \ln\left[\frac{I_{ji}\lambda_{ji}}{A_{ji}g_i}\right] = -\frac{E_j}{K_B T} + \mathrm{C} \tag{1}$$

Where:

(I_{ji}) the intensity,

(λ_{ji}) the wavelength,

(k_B) the Boltzmann constant,

(g_i) the statistical weight,

(A_{ji}) the probability of transition for spontaneous emission (*i* to *j* level),

(E_i) the excitation energy (eV),

(C) the Constant.

Can be used to determine the density of electron from the line width as Eq. (2), while the electron number density is often calculated using the Stark broadening [10]. The n_e is given by [11]:

$$n_e = \frac{\Delta\lambda\, FWHM}{2W_s} \times N_r \tag{2}$$

where: (n_e) the density of electron in cm^{-3}, (w_s) the theoretical line width, (Full Width at Half Maximum FWHM) $\Delta\lambda$ of the spectral line, (N_r) the reference electron density which calculate $\cong 10^{17} cm^{-3}$ for neutral atoms [12].

The length of Debye, or distance (λ_D), is given by [13]:

$$\lambda_D = \sqrt{\frac{\in_\circ K_B T_e}{n_e e^2}} = 743 \times \sqrt{\frac{T_e}{n_e}} \tag{3}$$

where:

(λ_D) the electron Debye length, ($\in_o$) permittivity of free space, (e) the charge of electron (C).

The no. of particles in the Debye-sphere (N_D) as dependent on density and temperature of electron [14]

$$N_D = \frac{4\pi}{3} n_e \lambda_D^3 = 1.38 \times 10^6 \frac{T_e^{3/2}}{n_e^{1/2}} \tag{4}$$

The frequency of plasma (w_{pe}), which described as [15]:

$$w_{p_e} = \sqrt{\frac{n_e e^2}{\in_\circ m_e}} = 8.98\sqrt{n_e} \tag{5}$$

Nanoscience, is a broad field of science that studies and uses different techniques to obtain stable and new means of nanoparticles compared to the original materials, nanoparticales become important due to their remarkable physical and chemical properties [16].

One of the primary goals of this work is to comprehend the processes that control the formation of plasma reactivity specie.

Experiment part

A simple design was employed to construct an atmospheric microwave induced plasma jet (MIPJ) system using readily available and inexpensive equipment procured from the local market. The microwave generator was operated at (w_{p_e} = 2.45 GHz) and coupled to a homemade tapered rectangular waveguide. Figure 1 shows the design of the atmospheric microwave induced plasma jet (MIPJ) system used in this study. The taper of the rectangular waveguide was varied from 72 mm to 5 mm to increase the electric field intensity in the region of interest, achieving an increase of about 2.6 times of the original value. A discharge tube made of quartz with different inner diameters (5–1 mm) and thicknesses was placed perpendicular to the waveguide and acted as an important barrier. The discharge tube was located 29 mm from the edge of the waveguide, where the electric field intensity is believed to reach its maximum, and had an open bottom end away from the waveguide surface. Integration of a UV-NIR spectrometer (S3000) into the system allowed direct recording of diagnostic data at different gas flow rates. Plasma spectroscopy analysis allowed the extraction of quantitative and qualitative information, including elemental composition. The electron density (ne) and temperature (T_e) of a plasma can be derived from the shape, wavelength, and fluctuations of the emission lines [17]. Of particular importance is the temperature (T_e) of a plasma, which is a key thermodynamic parameter because it can be used to characterize and predict various plasma properties, including the relative energy level distribution and particle velocity distribution.

Result and discussion

Diagnostic of argon gas flow rate

In Fig. 2 we see the intensity distribution of the plasma spectrum captured by the OES. The experimental setup consisted of 2.45 GHz argon (Ar) gas with discharge rates between 0.5 and 2 l/min and a voltage of (185) volts. Many Argon peaks are visible in the spectrum and most agree with

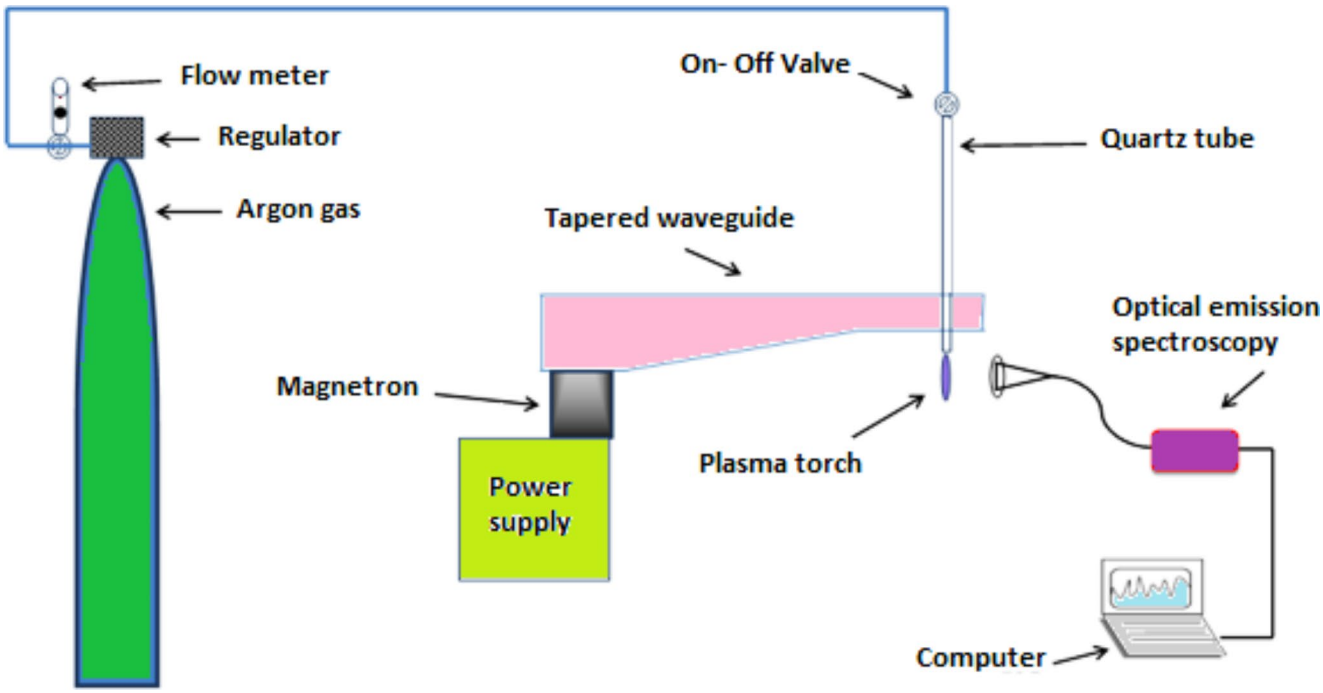

Fig. 1 Steps of work

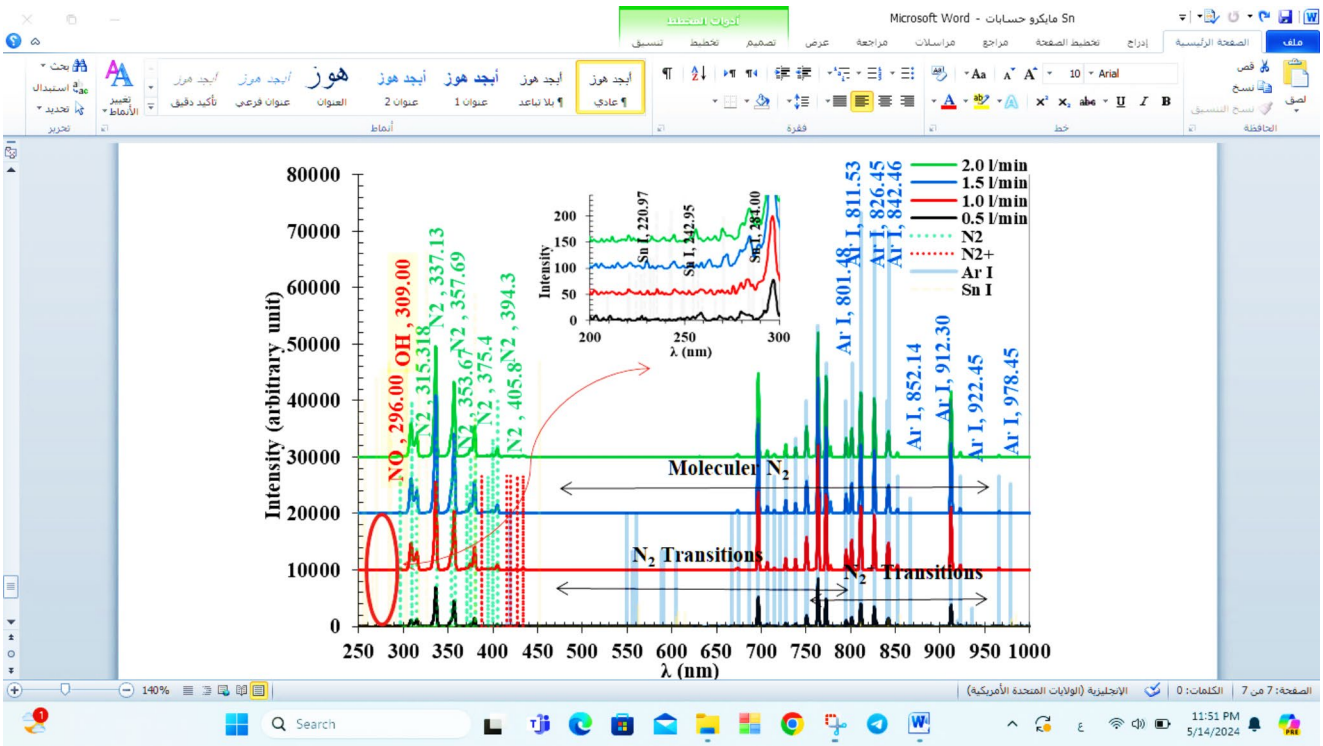

Fig. 2 Different levels of the argon gas flow rate (0.5-2 l/m) are characterized by a difference in intensity with respect to wavelength

NIST data [18]. Nitrogen (N2) absorbs in the range of 270 to 410 nm with a maximum at 337.13 nm. The Argon (ArI) spectrum always shows a maximum at 811.53 nm regardless of the gas flow rate. When the applied voltage was kept constant, the gas flow rate ranged from (1/2 to 2) l/min. Most of the plasma peaks were detected in the wavelength range of 200 to 1000 nm. It is clear that the emission of the ArI gas and the interaction intensity between the plasma

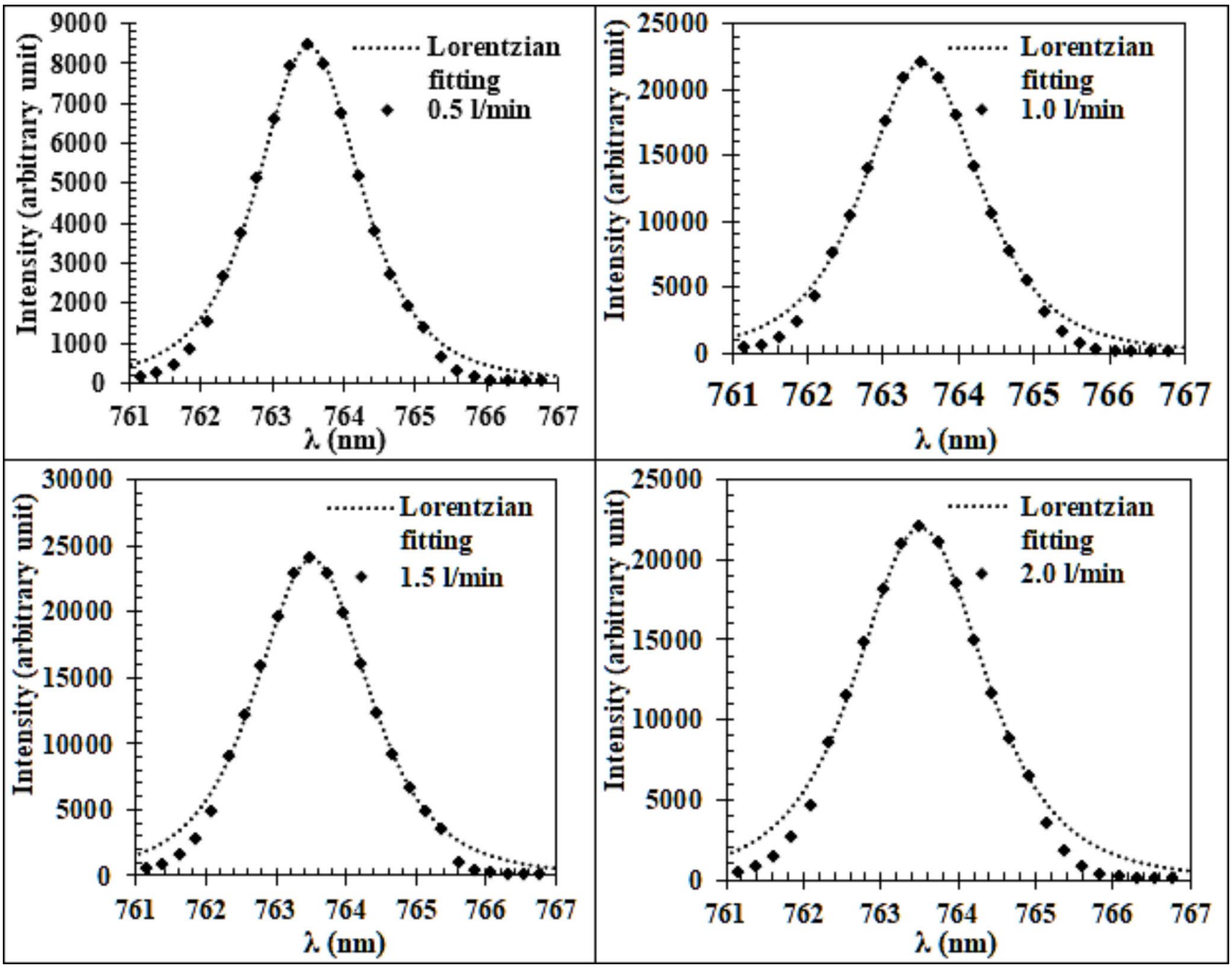

Fig. 3 The relationship between intensity and wavelength at the maximum apex for various flow rates of gas levels

particles increase. This finding is consistent with the work conducted by A. J. Mohamed and M. K. Khalaf [19]. Figure 2 shows the active plasma species produced by the argon gas in this system.

The spectrum of metallic tin (SnI) shows peaks in the range of (220.97–284.00) nm. Gas flows of 0.5 to 2 l/min and a constant applied voltage of 185 V were considered for the determination of these peaks. A study using NIST (National Institute of Standards and Technology) data showed that the maximum peak of (SnI) occurs at a plasma wavelength of (284.00) nm and a gas flow rate of (2) L/min. Figure 2 shows that the peak height increases with increasing gas flow rate. I know. Abbas and K.A.Aadim are right [20].

The following two figures measure temperature and electron number density, and the electron density (n_e) is obtained, calculated using Eq. (4), as shown in Fig. 3 [21]. Boltzmann plots the data of the most significant peak according to Eq. (1) and E, and the electron temperature (T_e) can be determined from the decay of the linear correspondence of the obtained curve, as shown in the Fig. 4.

As the gas flow rate increases at a constant applied voltage, as shown in Table 1, the results clearly show that the electron temperature increases by (0.485–0.583) eV and the electron density increases by (11.486×10^{17} -$13.176 \times 10^{17} cm^{-3}$. The correlation between the electron temperature and intensity in this system and the gas flow rate used to generate the plasma is shown in Fig. 5.

Table 1 parameters of a microwave plasma jet (MPJ) in Tin with several ranges of gas flow rates.

These results are consistent with those of (K.A. Aadim, G.H. Jihad) [22]. Gas molecules acquire energy from electrons. This means that there are more Argon molecules in the atmosphere and therefore more electrons to collide with gas atoms. The increased energy exchange from particles to gas atoms leads to an increase in the gas temperature. This process also primarily limits the electron emission from ions and atomic species in the Ar plasma. This means that

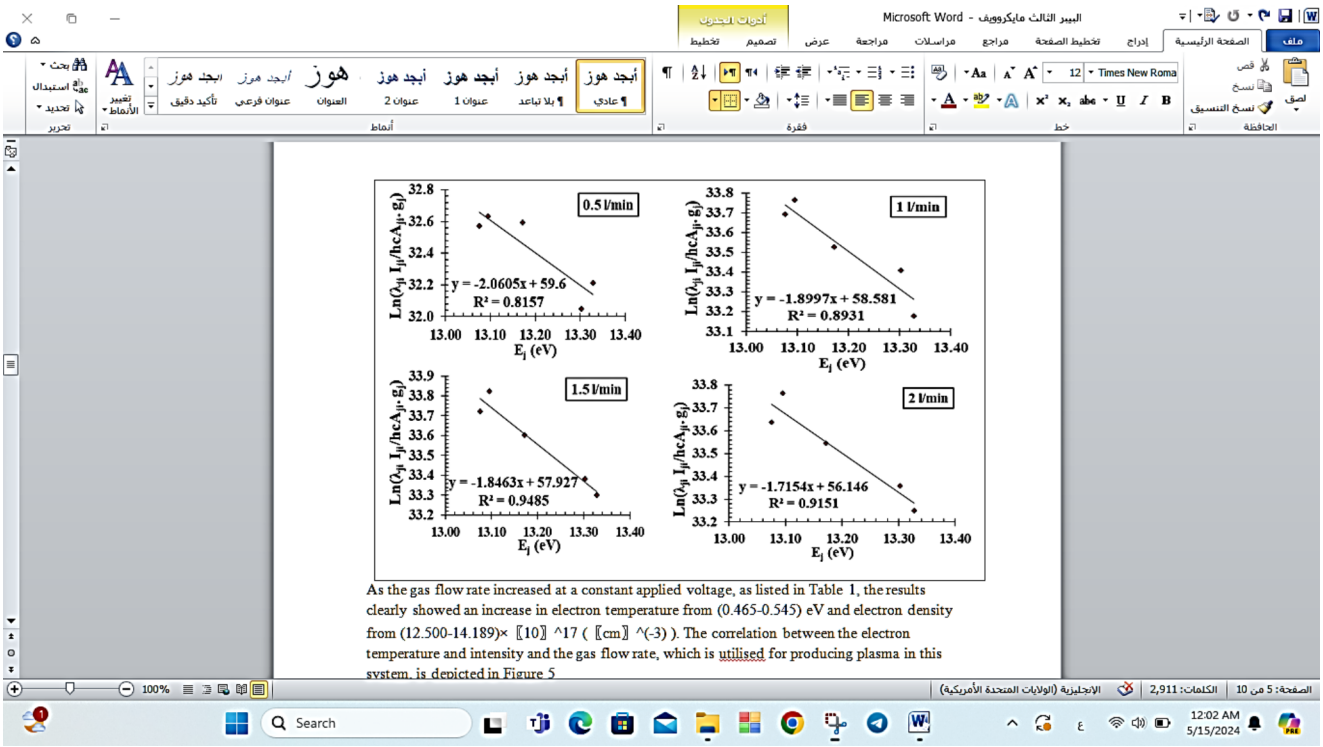

Fig. 4 Boltzmann plots for change values of gas flow-rate (0.5-2)l/min at the constant gas flow-rate of 5 l/min

Table 1 Parameters of a microwave plasma jet (MPJ) in Tin with several ranges of gas flow rates

Gas flow rate l/min	T_e (eV)	FWHM (nm)	n_e $\times 10^{17}$ (cm^{-3})	w_p $\times 10^{12}$ (Hz)	λ_D $\times 10^{-6}$ (cm)	N_d
0.5	0.485	1.700	11.486	9.624	4.830	542
1	0.526	1.800	12.162	9.903	4.888	595
1.5	**0.542**	**1.900**	**12.838**	**10.175**	**4.826**	**604**
2	**0.583**	**1.950**	**13.176**	**10.308**	**4.942**	**666**

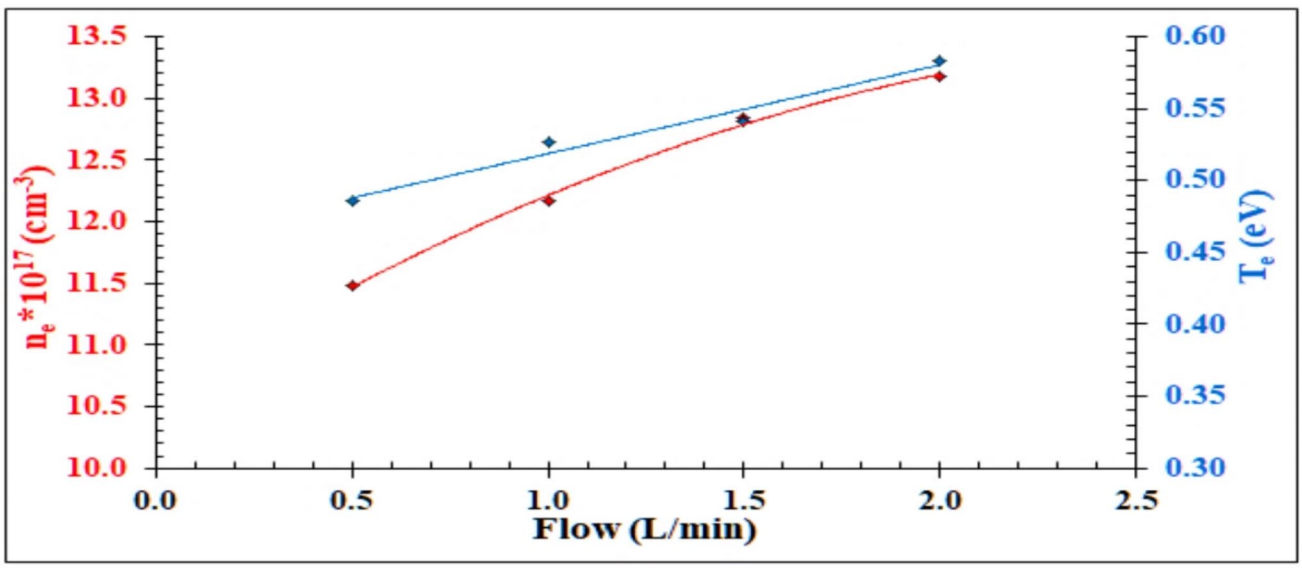

Fig. 5 Correlation between gas rate of flow (0.5-2) litres per minute and particle density and temperature

with increasing Argon flow rate, the lower energies in the electron energy distribution function become more prominent, while the higher energy tail decreases. Therefore, the electron density increases with flow rate due to the gradual ionization occurring inside the plasma jet tube.

In addition, a large fraction of the Argon (Ar) molecules passing through the plasma tube undergo tertiary ionization because the field potential is sufficient to induce such ionization. Therefore, the gas enters the plasma state as it passes through. Therefore, the electron density is lowest at 0.5 l/min and highest at 2 l/min, especially considering that the applied voltage is 185 kV; this indicates that an excess of Argon (Ar) is flowing through the plasma. The gas flow rate is directly related to the observed plasma properties. Neutral particles gain some electrons, while others lose them (neutral atoms). As can be seen in Fig. 5, the collapse process increases the electron density and temperature, which is triggered by the acceleration of the newly released electrons and the collision electrons of the external field. This process is called secondary ionization. The result is an increase in gas flow due to electrical failure. This is consistent with [23], as follows:

Absorbance spectra

As shown in Fig. 6, the UV-visible absorption spectrum of Sn nanoparticles is shown. The results show that the absorption increases with the increase of the gas flow measurement value. The absorption coefficient is calculated according to the following formula [24]

$$\alpha = 2.303\frac{A}{t} \tag{6}$$

Here, absorbance (A) and depth of film (t) are defined. More gas flow measurement readings meant more opportunities for the substance to be struck.

As can be seen in Fig. 7, the parameters of the prohibited energy gap, were determined using the equation that followed [25]:

$$\alpha\, hv = A(hv - E_g)^r \tag{7}$$

The symbol (E_g) denotes the forbidden potential gap, (hυ) denotes the energy of the photon and (A) remains constant.

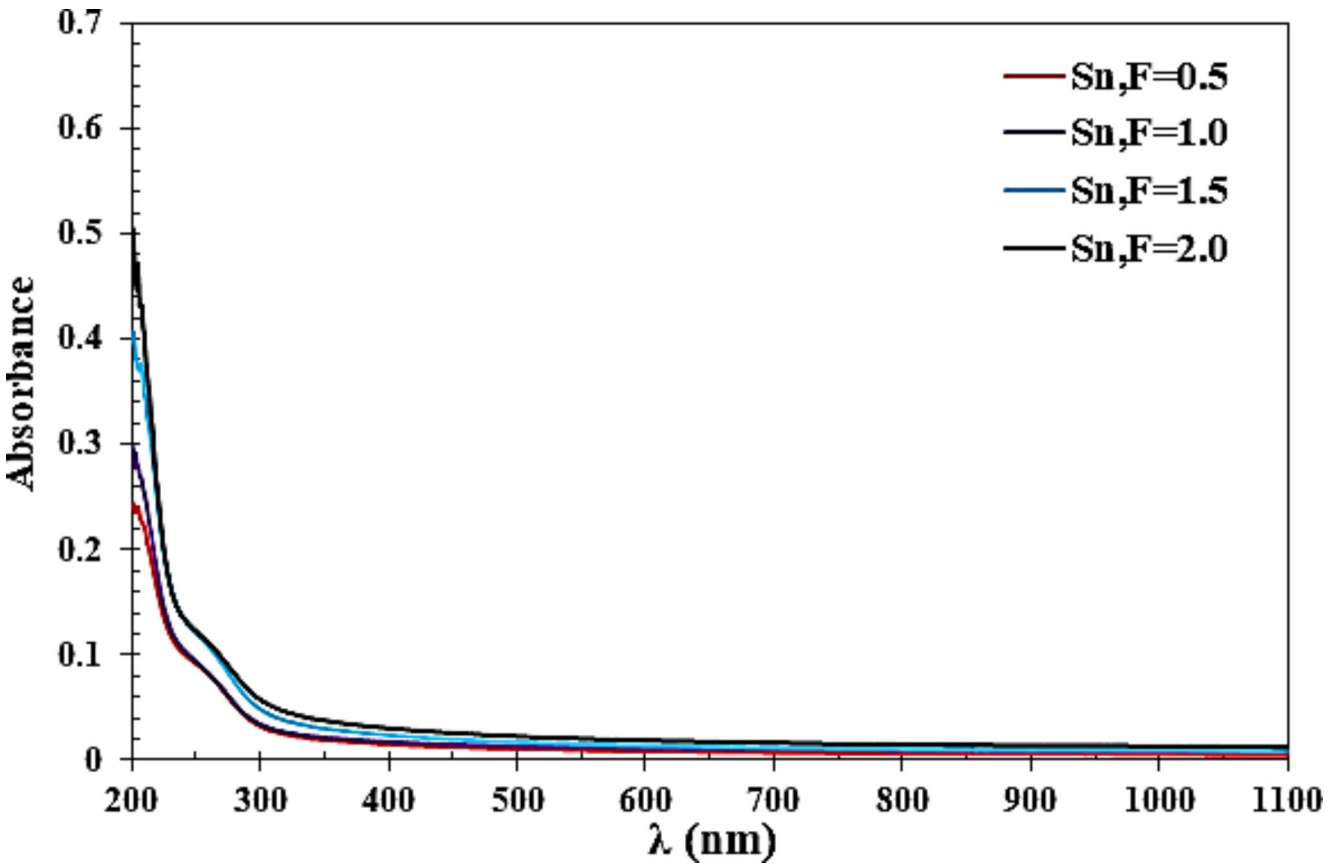

Fig. 6 The absorption spectra of thin coatings of Snproduced by a plasma jet at varying gas flow rates

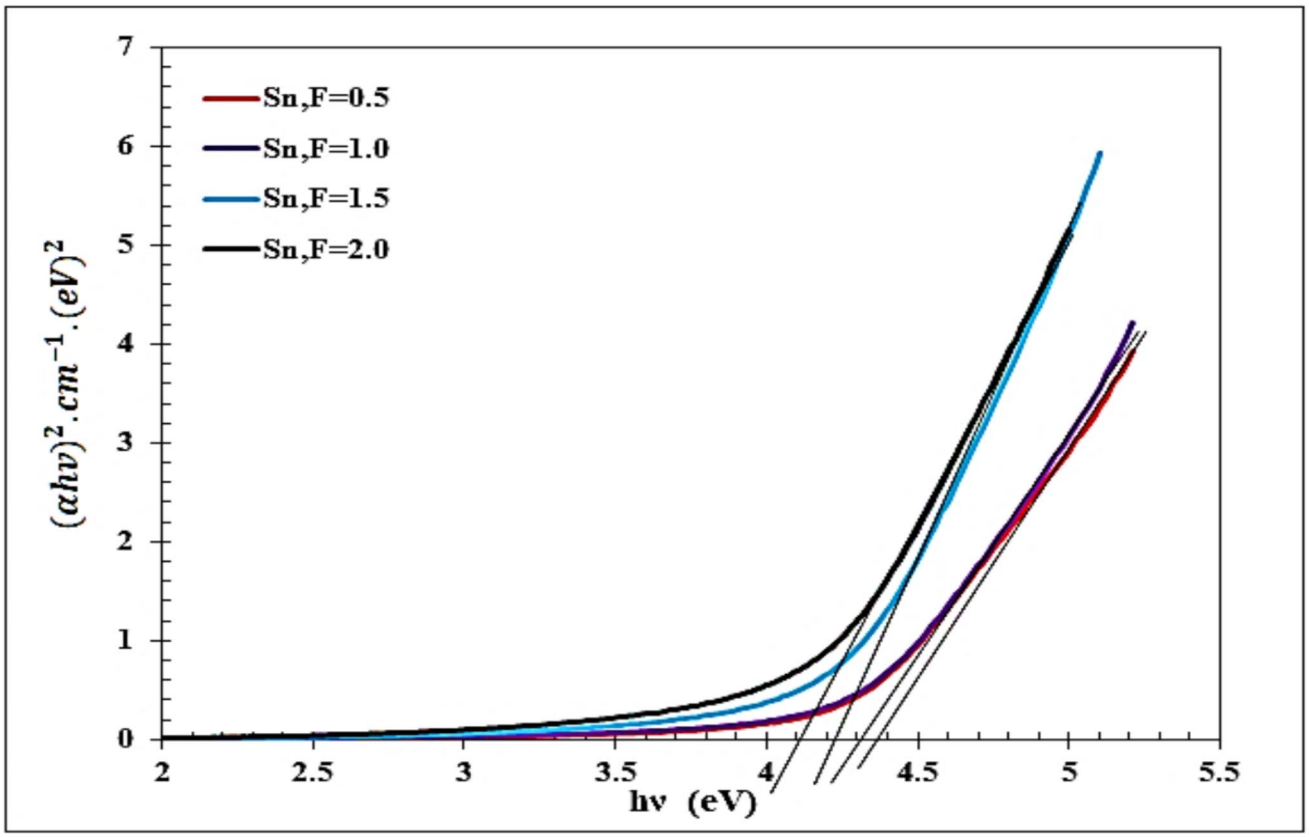

Fig. 7 Straightforward transition of SnO_2, produced by plasma jet at various gas flow rates

The value of the r coefficient varies depending on the type of transition: (1/2) denotes an allowed straight-line transition. An impermissible straight-line transition is denoted by (3/2) while an allowed transition is denoted by (2). Intermediate transitions and (3) denote forbidden intermediate transitions [26]. We note that the transition is direct, as shown in Fig. 7 and the observed decrease can be attributed to the fact that the material experiences more photon impacts due to the increase in gas flow rate. As a result, the material absorbs more photons, stimulating the generation of electrons and holes. Hence, the gap in the energy values decreases. The energy gap decreases from 4.4 eV to 4.1 eV can also be attributed to the manipulation of atomic dispersion and crystal phase transitions, as well as the material changes caused by the change in gas flow rate [27].

Conclusions

The generation of tin plasma using an atmospheric microwave plasma jet is an efficient, safe and cost-effective method for generating tin nanoparticles. The experiments found that the emission intensity increased with increasing gas flow rate. It is also worth noting that both the electron density (n_e) and the plasma frequency (w_{pe}) increased with increasing gas flow rate. On the other hand, the Debye length (λ_D) and the electron temperature (T_e) decreased with increasing gas flow rate. These findings demonstrate the effectiveness of nanoparticles in various fields, and the results show the effectiveness of nanoparticles in many fields, such as: B. Wound treatment and cancer treatment.

Acknowledgements This study would not have been possible without the help of the University of Baghdad's Plasma Physics Laboratory, Physics Department, and College of Science.

Declarations

Ethical approval The authors would like to declare that they do not have any conflict of interests.

References

1. D.V. Szabó, S. Schlabach, Microwave plasma synthesis of materials—from physics and chemistry to nanoparticles: a materials scientist's viewpoint. Inorganics. **2**(3), 468–507 (2014). https://doi.org/10.3390/inorganics2030468
2. H.J. Imran, K.A. Hubeatir, K.A. Aadim, A novel method for ZnO@NiO core–shell nanoparticle synthesis using pulse laser

ablation in liquid and plasma jet techniques. Sci. Rep. **13**(1), 5441 (2023). https://doi.org/10.1038/s41598-023-32330-z
3. N.K. Abdaalameer, S.N. Mazhir, K.A. Aadim, Diagnostics of zinc selenite plasma produced by FHG of a q-switchednd: Yaglaser. Chalcogenide Lett. **18**(7), 405–411 (2021). https://doi.org/10.15251/CL.2021.187.405
4. T. Shimizu, B. Steffes, R. Pompl, F. Jamitzky, W. Bunk, K. Ramrath, M. Georgi, W. Stolz, H.U. Schmidt, T. Urayama, S. Fujii, G.E. Morfill, Charact. Microw. Plasma Torch Decontamination Plasma Processes Polym. **5**, 577–582 (2008). https://doi.org/10.1002/ppap.200800021
5. J.H. Kim, Y.C. Hong, H.S. Kim, H.S. Kim, Simple microwave plasma source at atmospheric pressure. Journal-Korean Phys. Soc. **42**, S876–S879 (2003). https://doi.org/10.1016/j.wasman.2017.08.015
6. T.S. Hussein, A.F. Ahmed, K.A. Aadim, Spectroscopic analysis of CdO:Fe plasma generated by nd: YAG Laser. Iraqi J. Sci. **63**(2), 548–555 (2022). https://doi.org/10.24996/ijs.2022.63.2.12
7. R.K. Jamal, F.H. Ali, M.M. Hameed, K.A. Aadim, Designing a zener diode using ag. Iraqi J. Sci. **61**(5), 1032–1039 (2020). https://doi.org/10.24996/ijs.2020.61.5.12
8. D.T. Mohammed, G.H. Mohammed, Investigation of structural,optical and electrical properties of Mn doped with Cu thin films prepared by PLD tcchnique for slar cell applications. East. Eur. J. Phys. **3**, 391–399 (2023). https://doi.org/10.26565/2312-4334-2023-3-42
9. M.A. Khalaf, B.M. Ahmed, K.A. Aadim, Spectroscopic analysis of CdO1-X: SnX plasma produced by nd:YAG laser. Iraqi J. Sci. **61**(7), 1665–1671 (2020). https://doi.org/10.24996/ijs.2020.61.7.15
10. S.N. Mazhir, K.A. Aadim, M.M.F. Al-Halbosiy, N.K. Abdalameer, Cytotoxic activity of green zinc selenide nanoparticles against Hep-G2 cell lines. Indian J. Forensic Med. Toxicol. **15**(1), 2072–2078 (2021). https://doi.org/10.37506/ijfmt.v15i1.13713
11. A.A. Almaula, Ç.Y. Ataol, G.H. Mohammed, Structural and Optical Properties Study of SnS: Ag Doped Cu Thin films prepared by PLD technique for solar cell application. J. Pharm. Negat. Results. **13**(4), 936–944 (2022). https://doi.org/10.47750/pnr.2022.13.04.127
12. S.N. Rashid, K.A. Aadim, A.S. Jasim, A.M. Hamad, Synthesized Zinc Nanoparticles Via Pulsed laser ablation: characterization and antibacterial activity. Karbala Int. J. Mod. Sci. **8**(3), 462–476 (2022). https://doi.org/10.33640/2405-609X.3240
13. M.M. Shehab, K.A. Aadim, Spectroscopic diagnosis of the CdO:CoO plasma produced by nd:YAG laser Iraqi. J. Sci. **62**(9), 2948–2955 (2021). https://doi.org/10.24996/ijs.2021.62.9.11
14. A.J. Mohamed, M.K. Khalaf, A. Jasim, The study of the characteristics of a microwave plasma Jet Operated with Ar at Atmospheric pressure. Tikrit J. Pure Sci. **27**(4) (2022). https://doi.org/10.25130/tjps.27.2022.055
15. K.A. Aadim, A.Z. Mohammad, M.A. Abduljabbar, Influence of laser energy on synthesizes of CdO/Nps in liquid environment. IOP Conf. Ser. Mater. Sci. Eng. **454**, 012028 (2018). https://doi.org/10.1088/1757-899X/454/1/012028
16. R.S. Mohammed, K.A. Aadim, K.A. Ahmed, Spectroscopy Diagnostic of Laser Intensity Effect on Zn plasma parameters generated by nd:YAG Laser. Iraqi J. Sci. **63**(9), 3711–3718 (2022). https://doi.org/10.24996/ijs.2022.63.9.5
17. H.M. Abdulwahab, H.R. Humud, Plasma characterization of microwave plasma jet at Atmospheric pressure. Iraqi J. Sci. **65**(1), 151–159 (2024). https://doi.org/10.24996/ijs.2024.65.1.14
18. R.S. Mohammed, K.A. Aadim, K.A. Ahmed, Estimation of in vivo toxicity of MgO/ZnO core/shell nanoparticles synthesized by ecofriendly non-thermal plasma technology. Appl. Nanosci. **12**(12), 3783–3795 (2022). https://doi.org/10.1007/s13204-022-02608-1
19. D.Y. Khudair, A. Ansari, R.A. Tameem, M.K. Mohammed, G.H. Aadim, Impact of ZnO atomic ratio on structural, morphological and some optical properties of $(SnO_2)1_{-x}$ (ZnO)x thin films. Iraqi J. Sci. **61**(2), 333–340 (2020). https://doi.org/10.24996/ijs.2020.61.2.11
20. K.A. Aadim, Optical emission spectroscopic analysis of plasma parameters in tin–copper alloy co-sputtering system. Opt. Quant. Electron. **48**(12), 545 (2016). https://doi.org/10.1007/s11082-016-0820-7
21. R.T. Ahmed, A.F. Ahmed, K.A. Aadim, Influence of laser energy on structural and morphology properties of CdO and CdO: Sn production by laser-induced plasma, J. Opt. (India). **53**(2), 1564–1573 (2024). https://doi.org/10.1007/s12596-023-01291-x
22. K.A. Aadim, G.H. Jihad, Determination of electrons temperature and density for Ag, Zn, and Cu metals using plasma jet system at atmospheric pressure. Iraqi J. Sci., **63**(5), 2039–2047 (2022). https://doi.org/10.24996/ijs.2022.63.5.19
23. H. M. Abdulwahab, H.R. Humud, Plasma Characterization of Microwave Plasma jet at Atmospheric Pressure. Iraqi J. Sci. **65**(1), 151–159 (2024). https://doi.org/10.24996/ijs.2024.65.1.14
24. K.A. Aadim, Optical emission spectroscopic analysis of plasma parameters in tin–copper alloy co-sputtering system. Opt. Quantum. Electron. **48**(12), 545 (2016). https://doi.org/10.1007/s11082-016-0820-7
25. H.A. Abd El-Fattah, I.S. El-Mahallawi, M.H. Shazly, W.A. Khalifa, Optical properties and microstructure of tinxoy and tin thin films before and after annealing at different conditions. Coatings. **9**(1), 1–15 (2019). https://doi.org/10.3390/coatings9010022
26. M.N. Solovan, V.V. Brus, E.V. Maistruk, P.D. Maryanchuk, Electrical and optical properties of tin thin films. Inorg Materials. **50**(1), 40–45 (2014). https://doi.org/10.1134/S0020168514010178
27. R.K. Jamal, F.H. Ali, M.M. Hameed, K.A. Aadim, Designing A zener diode using Ag2O(1-X)Zno(X)/Psi structures deposited by laser induced plasma technique, Iraqi J. Sci. **61**(5), 1032–1039 (2020). https://doi.org/10.24996/ijs.2020.61.5.12